Analyzing Path Dependence in Final Modal User Equilibrium Using a Joint Trip-Length Distribution Framework

Namrata Gupta and Ludovic Leclercq

Univ Gustave Eiffel, ENTPE, EMob-lab, F-69675 Lyon, France

Keywords:
Congestion pricing; Multiple user equilibrium; Design history; Multimodal; Day-to-day dynamic traffic assignment; Trip-based MFD

Traditional transportation policy evaluations typically focus on the final state of User Equilibrium (UE), assuming it is unique and independent of the implementation process. However, in complex multimodal networks, this uniqueness is often undermined by cross-modal dynamics. This study provides a novel framework to model modal equilibrium by reformulating the problem through a joint probability distribution of trip-length tuples. By shifting the focus from individual origin-destination pairs to trip-length distributions, the framework significantly reduces computational complexity while maintaining spatial accuracy via a trip-based Macroscopic Fundamental Diagram (MFD).

We demonstrate the utility of this approach on the standard problem of designing and implementing pricing zones in dense urban areas. Taking Lyon, France, as a case study, we simulate the phased rollout of congestion pricing to observe the system's evolution. Our findings reveal that the final equilibrium state is inherently path-dependent: the specific sequence of implementation phases fundamentally alters the eventual modal split and network utilization levels. This research contributes both a computationally efficient methodology for multimodal modeling and empirical evidence that the sequence of policy interventions are as critical to urban planning as the final design itself.

1 Introduction

The evaluation of transportation policies often relies on how users react to it and modeled as User Equilibrium (UE), first formalized by Wardrop (1952). Wardrop's first principle states that equilibrium is reached when no traveler can unilaterally reduce their path cost. While Beckmann et al. (1956) and later Iryo

* Corresponding author. E-mail address: namrata.gupta@univ-eiffel.fr.

(2015) and Iryo and Smith (2018) demonstrated that a unique equilibrium (unicity) exists under conditions of convexity and strictly monotone travel time functions, these assumptions rarely hold in complex, modern urban networks. In Dynamic Traffic Assignment (DTA) and multimodal scenarios, the interaction between modes is often asymmetric—for instance, the presence of buses affects car speeds differently than cars affect buses—leading to an asymmetric Jacobian of the cost matrix (Mounce and Smith, 2007; Iryo and Watling, 2019; Ameli et al., 2022). Consequently, multiple equilibria can exist, and as Ameli et al. (2022) demonstrated, the sequence in which subway lines are introduced opened have significant influence on the final state of the system.

Solving DTA problems requires modeling congestion dynamics. To capture such dynamics at the urban scale, researchers have explored on the Macroscopic Fundamental Diagram (MFD) to tackle computational burden. Introduced by Daganzo (2007), the MFD describes a low-dimensional relationship between network vehicle accumulation and aggregate speed or outflow. This concept was later extended to trip-based MFD models (Mariotte et al., 2017; Lamotte and Geroliminis, 2018), which account for heterogeneity in trip lengths. Recent studies (Balzer and Leclercq, 2022; Balzer et al., 2023) have applied MFD-based approaches to solve modal equilibrium problems in the context of tradable credit schemes. Specifically, Balzer and Leclercq (2022) represents demand using tuples of origin, destination, and trip length, and employs a trip-based MFD to solve a static traffic assignment problem and optimize credit prices. Balzer et al. (2023) models demand as a distribution of car trip lengths and assumes an affine relationship between traffic variables of cars and Public Transportation (PT) to solve DTA and optimize time-based credit price. However, these approaches do not explicitly incorporate PT trip length distributions and lack a unified framework capable of handling more than two modes. This study addresses this limitation by formulating modal equilibrium as a joint probability distribution over modal trip lengths, thereby enabling a unified treatment of multimodal interactions. The framework is calibrated using data obtained from Google API services.

We utilize this framework to study the phased implementation of congestion pricing in Lyon, France. Most studies on optimization of tolls and Low Emission Zones (LEZ) do not account from phase implementation (Li et al., 2019; Yang et al., 2019; Chen et al., 2021). We argue that the path of implementation—how prices are revised or how infrastructure like mobility hubs are opened over time—is just as critical as the final design.

2 Methodological framework

2.1 The system

We consider a city center with a pricing-zone boundary. Private cars entering the zone incur a fee based on their departure time. To mitigate user inconvenience, mobility hubs are uniformly located along the boundary, enabling mixed-mode trips (car-to-PT transfers). The system initially includes two modes: cars and PT. The mixed mode becomes available only when parking hubs are opened. All hubs are opened simultaneously and, once opened, remain available.

The system involves two types of agents: the System Operator (SO) and users. The SO acts at discrete time intervals (e.g., every few days) and decides when to open parking hubs and how much to charge for access to the pricing zone. Users aim to minimize their individual travel costs. They choose among three modal options: car-only, PT-only, or a mixed trip (car to the boundary followed by PT).

Similar to Ameli et al. (2022), we consider a Day-to-Day adjustment (DTD) process in which a

fraction of users in a group update their modal choices based on their experience from the previous day. In case of unicity, this process converges to a single fixed point. However, when multiple equilibria exist, the converged state depends on the sequence of actions taken by the SO.

2.2 Demand representation

Consider an example city shown in Figure 1. The shaded area represents a pricing zone with a boundary equipped with (i) tolling infrastructure for private vehicles and (ii) mobility hubs (blue stars on the dashed boundary) where users can park and transfer to PT. A user with origin o and destination d has three modal options (m): car-only ($m = c$) (solid red arrows), PT-only ($m = p$) (solid green arrows), and mixed mode ($m = mx$) (dashed red and green arrows). Let l_{od}^{m} denote the expected trip length for mode m between o and d. For mixed trips, the total length is decomposed into a car leg ($l_{oh}^{mx,c}$) from origin to hub and a PT leg ($l_{hd}^{mx,p}$) from hub to destination.

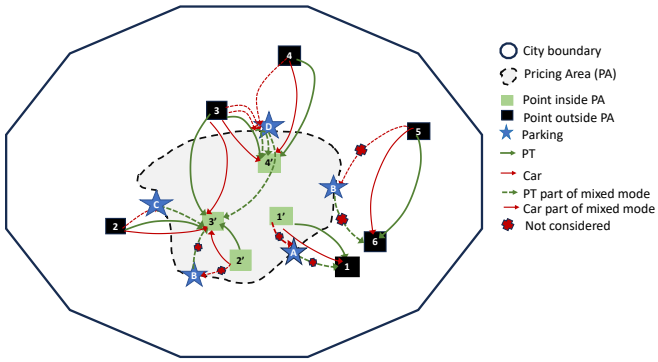


Figure 1: An example to visualize the problem

In Figure 1, we illustrate the available modal options for seven example OD pairs. The mixed mode is unrealistic when (i) both the origin and destination lie inside the pricing boundary (e.g., trip $2' \to 3'$), (ii) both lie outside it (e.g., trip $5 \to 6$), or (iii) the origin is inside and the destination is outside (e.g., trip $1' \to 1$). In such cases, users choose only between car and PT.

To represent demand, we model it as a joint probability density function (PDF) over modal trip lengths, $\phi_{\mathscr{L}^c,\mathscr{L}^p,\mathscr{L}^{mx,c},\mathscr{L}^{mx,p}}(\cdot)$, corresponding to car trip length, PT trip length, car leg of mixed trips, and PT leg of mixed trips. The demand between origin o and destination d is denoted by d_{od}.

Suppose that, in the considered example, some modal trip lengths are similar. For example, $l^c_{1'1} = l^c_{2'3'} = l^c_{23'} = l^c_{34'} = l^c_1$; $l^p_{1'1} = l^p_{2'3'} = l^p_{23'} = l^p_{34'} = l^p_1$; $l^{mx,c}_{2C} = l^{mx,c}_{3D} = l^{mx,c}_1$; and $l^{mx,p}_{C3'} = l^{mx,p}_{D4'} = l^{mx,p}_1$. The demand can then be aggregated into trip-length–based groups, as shown in Table 1. This aggregation reduces computational burden by collapsing the original seven OD pairs into five trip-length groups.

In practice, we discretize the joint PDF into N_b bins. Each bin b represents a tuple $\vec{l}_b = \{l^c_b, l^p_b, l^{mx,c}_b, l^{mx,p}_b\}$ and contains a fraction of the total demand. This reduces the problem complexity from $O(N^2)$ (where N is the number of nodes) to $O(N_b)$, where N_b is the number of unique trip-length combinations.

Equation (1) and Equation (2) give functional forms of the mixed-mode trip-length components. Here, $\bar{l}^c_{ob}$ and $\bar{l}^p_{bd}$ denote the average shortest distances from an origin to boundary by car and from the boundary to a destination by PT, respectively. The number of mobility hubs is denoted by n_h. α denotes circuity factor and $|B|$ is the perimeter of pricing boundary. Intuitively, as the number of hubs increases,

Table 1: Illustration of OD-to-trip-length aggregation under similarity in trip lengths assumptions.

OD Pair(s)	l^c	l^p	$(l^{mx,c}, l^{mx,p})$	**Aggregate Demand** (d_b)	**Assigned Bin** (b)
$(1',1),(2',3')$	l^c_1	l^p_1	$(0,0)$	$d_{1'1}+d_{2'3'}$	1
$(5,6)$	l^c_{56}	l^p_{56}	$(0,0)$	d_{56}	2
$(2,3'),(3,4')$	l^c_1	l^p_1	$(l^{mx,c}_1, l^{mx,p}_1)$	$d_{23'}+d_{34'}$	3
$(3,3')$	$l^c_{33'}$	$l^p_{33'}$	$(l^{mx,c}_1, l^{mx,p}_{D3'})$	$d_{33'}$	4
$(4,4')$	$l^c_{44'}$	$l^p_{44'}$	$(l^{mx,c}_{4D}, l^{mx,p}_1)$	$d_{44'}$	5

vehicles require less detour to reach a hub before transferring to PT. Consequently, as $n_h \to \infty$, $l^{mx,c}_{oh} \to \bar{l}^c_{ob}$ and $l^{mx,p}_{hd} \to \bar{l}^p_{bd}$.

$$l^{mx,c}_{oh} = \bar{l}^c_{ob} + \alpha \frac{|B|}{2n_h} \tag{1}$$

$$l^{mx,p}_{hd} = \bar{l}^p_{bd} + \alpha \frac{|B|}{2n_h} \tag{2}$$

To summarize, we group travelers with similar modal trip lengths and departure time. So, for each demand group i, $d_i := d(\vec{l}_i, t_{d_i})$, the modal shares $(0 \le x^m_i \le 1,\ m \in \{c,p,mx\})$ is obtained as the solution of UE. Here, $\vec{l}_i = \{l^c_i, l^p_i, l^{mx,c}_i, l^{mx,p}_i\}$ and t_{d_i} is the departure time of group i.

2.3 Aggregate demand calibration

We calibrate the joint distribution of trip length using Google API services. This process is divided into four stages: spatial harvesting, gateway identification, multi-modal feature extraction, and demand estimation for a given joint distribution.

2.3.1 Spatial Harvesting of OD Locations

Using the OSMnx (Boeing, 2017) and Google Places API (Google, 2024c), we define the administrative boundary of desired city and surrounding municipalities as Suburbs. We harvest Points of Interest (POIs) across ten categories, such as transit stations, shopping malls, and universities, to ensure diversity in trip lengths. Since $m = mx$ is feasible only when origin is outside boundary and destination is inside boundary, origins are filtered to remain strictly outside the city boundary, while destinations are constrained within the core.

2.3.2 Mixed-Mode Gateway Identification

A key contribution of this model is the explicit routing of mixed-mode trips through mobility hubs. To identify the optimal transition point for each OD pair, we extract the city boundary as a sequence of network nodes from OSM. For each origin O, we identify a boundary gateway BG by solving a multi-source Dijkstra's algorithm on the projected road network. The gateway BG is selected as the boundary

node that minimizes the car distance from the origin, as shown in Equation (3). Here, $\mathscr{B}$ is boundary nodes set. This point BG is used to calculate shortest distances to boundary.

$$BG = \arg\min_{b \in \mathscr{B}} \{\text{dist}(O, b)\} \tag{3}$$

2.3.3 Multi-modal Feature Extraction

For each of the given number of OD pairs, we perform parallelized queries to the Google Maps Distance Matrix (Google, 2024a) and Directions (Google, 2024b) APIs. We extract distances and free-flow travel times for three distinct paths: (i) car route length from O to D (l^c), (ii) PT (bus, tram, or subway) route length from O to D (l^p), (iii) mixed-Mode ($l^{mx,c}, l^{mx,p}$): car leg from O to BG and a transit leg from BG to D. The resulting dataset provides the four-dimensional tuple $\vec{l_i} = \{l_i^c, l_i^p, l_i^{mx,c}, l_i^{mx,p}\}$ for every group i.

2.3.4 Demand Discretization and Empirical Calibration

We first estimate the underlying joint probability density of our harvested OD pairs using a multi-variate KDE (Equation (4)). Here, K is the Gaussian kernel and $\mathbf{h}$ is the bandwidth. We then evaluate this density at the centers of a 4D grid, where each dimension is binned according to predefined lengths ($\Delta l^c, \Delta l^p, \Delta l^{mx,c}, \Delta l^{mx,p}$). This yields a weight for every possible trip-length combination.

$$\hat{f}(\vec{l}) = \frac{1}{n\mathbf{h}} \sum_{j=1}^{n} K\left(\frac{\vec{l} - \vec{l}_j}{\mathbf{h}}\right) \tag{4}$$

The total demand for each time-slice is scaled to match real-world observations ($d_{total,t}^{real}$). Finally, we assign random departure times to each group.

2.4 Estimating travel cost using trip-based MFD simulation

The generalized cost of mode $m \in \mathscr{M}$ for group i depends on its travel time (TT_i^m) and the associated price P_i^m. For simplicity, we consider only congestion pricing, i.e., $P_i^p = P_i^{mx} = 0$, and P_i^c represents the charge set by the SO at the departure time of group i. Equations (5) to (7) define the modal travel costs. γ denotes the Value of Time (VOT).

$$TC_i^c = \gamma TT_i^c + P_i^c \tag{5}$$
$$TC_i^p = \gamma TT_i^p \tag{6}$$
$$TC_i^{mx} = \gamma TT_i^{mx} = \gamma(TT_i^{mx,c} + TT_i^{mx,p}) \tag{7}$$

Travelers in group i using mode m traverse trip length l_i^m with a mean speed $V_i^m(t)$. Users are labeled active for the interval $t_{d_i} \leq t \leq t_{d_i} + TT_i^m$. The trip length and travel time satisfy Equation (8). The car speed satisfy MFD constraint (Equation (11)), while the PT speed follows an affine relationship with car speed (Equation (12)). Here, β_2 represents the base speed of PT (reflecting dedicated infrastructure in case of dedicated bus lines, trams or subways), and β_1 accounts for the interference factor from car traffic.

In simulation, the car accumulation $n^c(t)$ is computed by aggregating all travelers using the car network at time t, as shown in Equation (13). Mixed-mode users contribute to $n^c(t)$ only during their car leg; upon reaching a mobility hub, they exit the car network and transition to the PT network. The modal travel time TT_i^m is determined by identifying the time at which travelers in group i complete the total distance l_i^m.

$$l_i^m = \int_{t_{d_i}}^{t_{d_i}+TT_i^m} V_i^m(t)dt \; m \in \{c, p\} \tag{8}$$

$$l_i^{mx,c} = \int_{t_{d_i}}^{t_{d_i}+TT_i^{mx,c}} V_i^c(t)dt \tag{9}$$

$$l_i^{mx,p} = \int_{t_{d_i}+TT_i^{mx,c}}^{t_{d_i}+TT_i^{mx,c}+TT_i^{mx,p}} V_i^p(t)dt \tag{10}$$

$$V_i^c(t) = V_i^c(n^c(t)) \tag{11}$$

$$V_i^p(t) = \beta_1 V_i^c(n^c(t)) + \beta_2 \tag{12}$$

$$n^c(t) = \sum_i \sum_{m \in \{c, mx\}} x_i^m \cdot \mathbf{1}_{\text{car phase active at } t} \tag{13}$$

2.5 User equilibrium

The system reaches Modal UE when, for every demand group i, no traveler can reduce their generalized travel cost by unilaterally switching modes. Following the first principle of Wardrop (1952), Equation (14) gives the equilibrium conditions for each demand group i.

$$\begin{cases} TC_i^m = \min_{k \in \mathscr{M}}\{TC_i^k\}, & \text{if } x_i^m > 0 \\ TC_i^m \geq \min_{k \in \mathscr{M}}\{TC_i^k\}, & \text{if } x_i^m = 0 \end{cases} \tag{14}$$

To achieve UE, we implement DTD process that mimics the behavioral adjustment of travelers over maximum number of days ($D_{\max}$). At each day d, users evaluate the experienced cost of their chosen mode against the available alternatives at day $d-1$. The transition of modal shares is governed by a switching probability P_{swap} from non-optimal mode m to better mode (Equation (15)) and a constant adjustment rate μ. Equation (16) gives the fraction of user that leaves non-optimal mode m and shifts to the mode with minimum cost.

$$P_{swap,i}^m = \frac{TC_i^m - \min_k\{TC_i^k\}}{TC_i^m} \tag{15}$$

$$\Delta x_i^m = x_i^m \cdot P_{swap,i}^m \cdot \mu \tag{16}$$

The convergence of the system toward equilibrium is monitored using the Average Relative Gap (AG^d), defined as the demand-weighted excess cost across all groups and modes (Equation (17)). The process terminates when (i) $D_{\max}$ is achieved, or (ii) AG^d fall below a predefined threshold ε. Whenever

SO changes the system, the modal fraction from the previous day becomes the initial state for the next phase.

$$AG^d = \frac{\sum_i d_i \sum_{m \in \mathscr{M}} x_i^m (TC_i^m - \min_k \{TC_i^k\})}{\sum_i d_i} \tag{17}$$

2.6 Assumptions

To ensure the analytical tractability of the framework, the following assumptions are adopted:

- The urban area is modeled as a single homogeneous region where a well-defined car MFD exists. The car MFD is independent of PT operations, and an affine relationship exists between the average speeds of both modes.
- The pricing-zone boundary is fixed.
- Total demand remains constant. While users may switch modes in response to pricing and congestion, trip cancellation and departure time shifts are not considered.
- All travelers have universal access to all the considered modes. Mixed-mode is available once SO decides to open them.
- The period of decision of SO is sufficient for the DTD process to reach a stable UE.

3 Case study

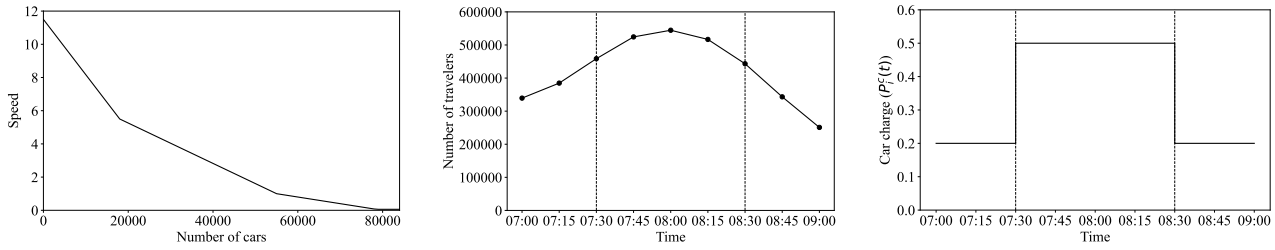
3.1 Experimental setup

The experimental framework focuses on the Lyon metropolitan area, France, modeled as the core congestion pricing zone. To characterize network performance, we employ a car MFD experimentally calibrated by Mariotte et al. (2020), as illustrated in Figure 2a. Suburban-urban travel dynamics are captured by selecting 23 surrounding municipalities as origin points for the trip-length distributions.Table 2 summarizes the key model parameters. β_1 and β_2 are adopted from Balzer et al. (2023).

The temporal demand profile is shown in Figure 2b, with departure times ranging from 7:00 AM to 9:00 AM. To evaluate policy interventions, SO designates the window between 7:30 AM and 8:30 AM as the peak period, during which higher congestion charges are applied. Although the baseline VOT is set at $\gamma = 1$ €/h, we conducted a sensitivity analysis for higher VOT values; the resulting trends and the existence of path dependence remained consistent across these variations. The simulation terminates once all traveler groups have completed their respective trip lengths within the joint distribution framework.

The SO manages the system through five possible actions, all of which are irreversible. Decisions are implemented every 200 days, and multiple actions may be applied simultaneously:

- A_1 **(Infrastructure):** Opening of parking hubs to facilitate modal transfers. Without this action $m = mx$ is infeasible



(a) Car MFD calibrated in Mariotte et al. (2020)

(b) Demand

(c) Final charges set by SO

Figure 2: Considered traffic scenario

Table 2: Model Parameters

Parameter	**Symbol**	**Value**
Harvested OD pairs	N_{OD}	5,000
Search radius	R	30 km
KDE bandwidth	h	0.5
PT interference factor	β_1	1.2
PT base speed	β_2	3.17 km/h
Value of time (VOT)	γ	1 €/h
Adjustment rate	μ	0.1
Convergence threshold	ε	10^{-3}
SO decision time step	$D_{\max}$	200 days

Table 3: Implementation sequences for infrastructure and pricing interventions.

Sequence	**Day 0**	**Day 200**	**Day 400**	**Day 600**	**Day 800**	**Final UE**
S_1 (Shock)	A_1, A_3, A_5	—	—	—	—	$I \to F_1$
S_2 (Infra-First)	A_1	A_2	A_3	A_4	A_5	F_2
S_3 (Price-First)	A_2	A_3	A_4	A_5	A_1	F_3
S_4 (Hybrid)	A_2	A_1	A_3	A_4	A_5	F_4

- A_2 **(Peak Pricing I):** Introduction of a 0.2 € congestion charge during the peak period.
- A_3 **(Peak Pricing II):** Escalation of the peak period congestion charge to 0.5 €.
- A_4 **(Off-Peak Pricing I):** Introduction of a 0.1 € congestion charge during the off-peak period.
- A_5 **(Off-Peak Pricing II):** Escalation of the off-peak congestion charge to 0.2 €.

To investigate path dependence, we define four distinct implementation sequences that start from a common initial equilibrium between car and PT users (Point I) and converge toward an identical final policy configuration, as summarized in Table 3. By comparing the respective final states (F_1–F_4), we assess whether the sequence of policy implementation affects long-term modal shares and network performance.

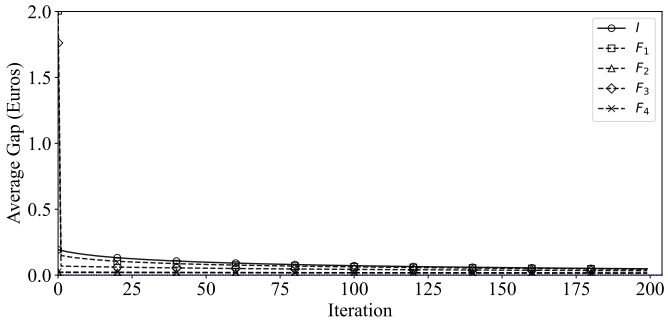


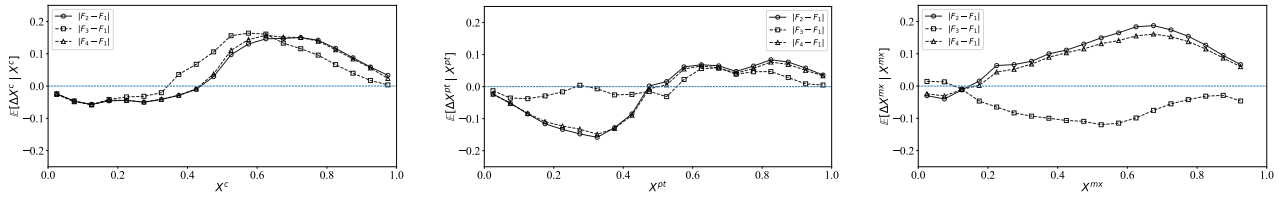
Figure 3: Quality of convergence through average gap

3.2 Results

To ensure the reliability of the observed path dependence, we examine the stability of the equilibrium solutions. Figure 3 illustrates the evolution of the average convergence gap across the decision periods for each sequence. The final gap values for all sequences are consistently low and comparable. This indicates that each sequence reaches a stable UE, confirming that the divergent states (F_1 through F_4) are not artifacts of numerical instability but represent distinct, converged equilibrium points.

We now analyze the deviation between the final UE of different sequences compared to the reference sequence S_1. Figure 4 and Figure 5 illustrate the conditional mean differences in modal outcomes relative to the reference scenario (F_1) as a function of modal shares and departure times, respectively.

In Figure 4, a clear divergence is observed between S_3 (Price-First) and the other sequences. S_3 consistently shows a negative deviation in car usage. This suggests that implementing pricing before infrastructure creates a more significant deterrent to car use that persists even after mobility hubs are later introduced. Conversely, S_2 (Infra-First) and S_4 (Hybrid) exhibit similar trends, often showing higher car retention compared to S_1, indicating that providing car-friendly infrastructure early in the rollout may dampen the eventual impact of congestion charges.

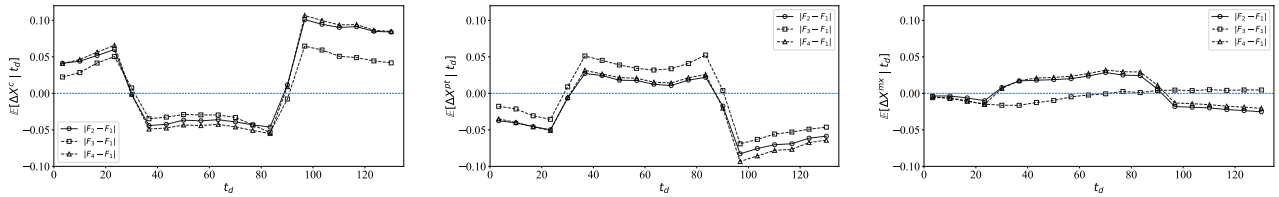


(a) Car **(b)** PT **(c)** Mix

Figure 4: Conditional mean deviation between scenarios (F_2, F_3, F_4) and the reference (F_1) as a function of modal share

The temporal analysis in Figure 5 reveals that the most significant deviations occur during the peak period (7:30 AM – 8:30 AM). S_3 exhibits a higher reduction in car travel and an increase in PT during this window. Interestingly, S_2 and S_4 show a rebound effect in the latter half of the peak period, where car usage deviations become positive. This implies that the sequence of interventions does not just change the magnitude of the modal shift, but fundamentally reshapes the temporal distribution of demand across the network.

The cumulative impact of these trajectories is summarized in Figure 6, which presents the difference in Total Travel Time (TTT) for each mode. S_3 (Price-First) results in a substantial reduction in TTT for



(a) Car **(b)** PT **(c)** Mix

Figure 5: Conditional mean deviation between scenarios (F_2, F_3, F_4) and the reference (F_1) as a function of departure time

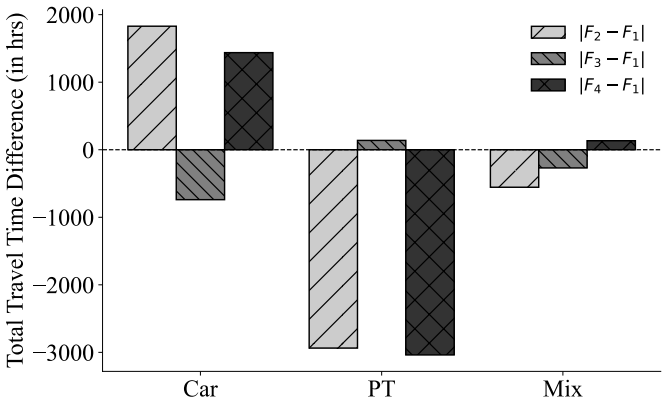


Figure 6: Difference in total travel time of modes

cars and a slight increase for PT.

4 Conclusion

This study demonstrates that in multimodal networks, the path toward policy implementation is as influential as the final design itself. By employing a joint trip-length distribution framework and a trip-based MFD, we evaluated the evolution of the Lyon network under four distinct intervention sequences. Our findings provide empirical evidence of path dependence in final modal UE.The results highlight a critical trade-off for urban planners: the Price-First sequence (S_3) proved most effective at suppressing car travel and reducing network-wide total travel time. In contrast, Infrastructure-First (S_2) or Hybrid (S_4) strategies, while intuitively supportive of modal shifts, can inadvertently lock-in higher levels of car dependency if the infrastructure (mobility hubs) is introduced before sufficient fiscal deterrents are in place.

References

Ameli, M., Lebacque, J. P., and Leclercq, L. (2022). Evolution of multimodal final user equilibrium considering public transport network design history. *Transportmetrica B: Transport Dynamics*, 10(1):923–953.

Balzer, L., Ameli, M., Leclercq, L., and Lebacque, J.-P. (2023). Dynamic tradable credit scheme for multimodal urban networks. *Transportation Research Part C: Emerging Technologies*, 149:104061.

Balzer, L. and Leclercq, L. (2022). Modal equilibrium of a tradable credit scheme with a trip-based MFD and logit-based decision-making. *Transportation Research Part C: Emerging Technologies*, 139:103642.

Beckmann, M., McGuire, C. B., and Winsten, C. B. (1956). STUDIES IN THE ECONOMICS OF TRANSPORTATION.

Boeing, G. (2017). Osmnx: New methods for acquiring, constructing, analyzing, and visualizing complex street networks. *Computers, Environment and Urban Systems*, 65:126–139.

Chen, Y., Zheng, N., and Vu, H. L. (2021). A novel urban congestion pricing scheme considering travel cost perception and level of service. *Transportation Research Part C: Emerging Technologies*, 125:103042.

Daganzo, C. F. (2007). Urban gridlock: Macroscopic modeling and mitigation approaches. *Transportation Research Part B: Methodological*, 41(1):49–62.

Google (2024a). Distance matrix api. `https://developers.google.com/maps/documentation/distance-matrix`. Accessed: 2026-04-14.

Google (2024b). Distance matrix api. `https://developers.google.com/maps/documentation/Directions`. Accessed: 2026-04-14.

Google (2024c). Google maps platform. `https://developers.google.com/maps`. Accessed: 2026-04-14.

Iryo, T. (2015). Investigating Factors for Existence of Multiple Equilibria in Dynamic Traffic Network. *Networks and Spatial Economics*, 15(3):599–616.

Iryo, T. and Smith, M. J. (2018). On the uniqueness of equilibrated dynamic traffic flow patterns in unidirectional networks. *Transportation Research Part B: Methodological*, 117:757–773.

Iryo, T. and Watling, D. (2019). Properties of equilibria in transport problems with complex interactions between users. *Transportation Research Part B: Methodological*, 126:87–114.

Lamotte, R. and Geroliminis, N. (2018). The morning commute in urban areas with heterogeneous trip lengths. *Transportation Research Part B: Methodological*, 117:794–810.

Li, Y., Guo, Y., Lu, J., and Peeta, S. (2019). Impacts of congestion pricing and reward strategies on automobile travelers' morning commute mode shift decisions. *Transportation Research Part A: Policy and Practice*, 125:72–88.

Mariotte, G., Leclercq, L., Batista, S. F. A., Krug, J., and Paipuri, M. (2020). Calibration and validation of multi-reservoir MFD models: A case study in Lyon. *Transportation Research Part B: Methodological*, 136:62–86.

Mariotte, G., Leclercq, L., and Laval, J. A. (2017). Macroscopic urban dynamics: Analytical and numerical comparisons of existing models. *Transportation Research Part B: Methodological*, 101:245–267.

Mounce, R. and Smith, M. (2007). *Uniqueness of equilibrium in steady state and dynamic traffic networks*, volume 17. Elsevier.

Wardrop, J. G. (1952). ROAD PAPER. SOME THEORETICAL ASPECTS OF ROAD TRAFFIC RESEARCH. *Proceedings of the Institution of Civil Engineers*, 1(3):325–362.

Yang, D.-x., Qiu, L.-s., Yan, J.-j., Chen, Z.-y., and Jiang, M. (2019). The government regulation and market behavior of the new energy automotive industry. *Journal of Cleaner Production*, 210:1281–1288.